Available online at www.sciencedirect.com
ScienceDirect
Biochimica et Biophysica Acta 1767 (2007) 1233–1244
Biochimica et Biophysica Acta
BBA
www.elsevier.com/locate/bbabio

The thylakoid proton motive force *in vivo*. Quantitative, non-invasive probes, energetics, and regulatory consequences of light-induced *pmf*

Kenji Takizawa, Jeffrey A. Cruz, Atsuko Kanazawa, David M. Kramer *

Institute of Biological Chemistry, 289 Clark Hall, Washington State University, Pullman, WA 99164-6340, USA

Received 29 March 2007; received in revised form 26 June 2007; accepted 3 July 2007
Available online 24 July 2007

Abstract

Endogenous probes of light-induced transthylakoid proton motive force (*pmf*), membrane potential ($\Delta\psi$) and ΔpH were used *in vivo* to assess in *Arabidopsis* the lumen pH responses of regulatory components of photosynthesis. The accumulation of zeaxanthin and protonation of PsbS were found to have similar pK_a values, but quite distinct Hill coefficients, a feature allowing high antenna efficiency at low *pmf* and fine adjustment at higher *pmf*. The onset of "energy-dependent' exciton quenching (q_E) occurred at higher lumen pH than slowing of plastoquinol oxidation at the cytochrome b_6f complex, presumably to prevent buildup of reduced electron carriers that can lead to photodamage. Quantitative comparison of intrinsic probes with the electrochromic shift signal *in situ* allowed quantitative estimates of *pmf* and lumen pH. Within a degree of uncertainly of ~0.5 pH units, the lumen pH was estimated to range from ~7.5 (under weak light at ambient CO_2) to ~5.7 (under 50 ppm CO_2 and saturating light), consistent with a 'moderate pH' model, allowing antenna regulation but preventing acid-induced photodamage. The apparent pK_a values for accumulation of zeaxanthin and PsbS protonation were found to be ~6.8, with Hill coefficients of about 4 and 1 respectively. The apparent shift between *in vitro* violaxanthin deepoxidase protonation and zeaxanthin accumulation *in vivo* is explained by steady-state competition between zeaxanthin formation and its subsequent epoxidation by zeaxanthin epoxidase. In contrast to tobacco, *Arabidopsis* showed substantial variations in the fraction of *pmf* (0.1–0.7) stored as $\Delta\psi$, allowing a more sensitive qE response, possible as an adaptation to life at lower light levels.

Keywords: Chloroplast; Cytochrome b6f complex; Electrochromic shift; In vivo spectroscopy; Non-photochemical quenching; Regulation of photosynthesis

1. Introduction

In higher plant photosynthesis, light-driven electron transfer stores energy in an electrochemical gradient of protons, termed the proton motive force (*pmf*). The total *pmf*, consisting of the sum of membrane potential ($\Delta\psi$) and proton diffusion potential (ΔpH), is used to drive ATP synthesis at the CF_O-CF_1-ATP synthase (ATP synthase) [1], while acidification of the thylakoid lumen caused by the ΔpH component acts as a key signaling component, regulating light capturing, via the 'energy-dependent' quenching (q_E) mechanism, which dissipates 'excess' light energy harmlessly as heat (reviewed in [2]). q_E is distinguished from other non-photochemical quenching processes by its distinctive mode of activation (i.e. by acidification of the lumen), its relaxation behavior in the dark and its strict correlation to the appearance of absorbance changes at 535 nm.

The initiation of q_E involves two lumen pH-dependent processes, the activation of violaxanthin deepoxidase (VDE) which converts violaxanthin (V) to antheraxanthin (A) and A to zeaxanthin (Z) and the protonation of PsbS, a protein component of the photosystem II antenna complex. In addition, acidification of the lumen slows the oxidation of plastoquinol (PQH_2) at the cytochrome (cyt) b_6f complex, thus regulating overall electron transfer [3].

Currently, there is a great deal of interest in understanding photosynthesis as a complete "system" in order to predict the responses of photosynthesis to environmental changes. It is clear that the light reactions and downstream biochemical processes are tightly integrated to balance photochemical efficiency with avoidance of photodamage and that the *pmf* plays a central role in this integration (reviewed in [4]). In this context, given the central importance of thylakoid *pmf* in sustaining and

* Corresponding author. Fax: +1 509 335 7643.
E-mail address: dkramer@wsu.edu (D.M. Kramer).

0005-2728/$ - see front matter © 2007 Elsevier B.V. All rights reserved.
doi:10.1016/j.bbabio.2007.07.006

regulating photosynthesis, it is critical that we have the ability to probe it *in vivo*. Extrapolating from *in vitro* studies is risky, as illustrated by early work suggesting that all *pmf* is stored as ΔpH, implying a highly acidic lumen (ΔpH ~3.5, reviewed in [5]). More recent work has argued that such an acidic lumen is incompatible with the known properties of the photosynthetic machinery (reviewed in [4,5]). Low lumen pH can severely slow key electron transfer processes, particularly plastoquinol oxidation at the cyt b_6f complex [6,7], and sensitize photosystem (PS) II to photodamage [8]. Instead, we suggested that lumen pH remains moderate, above about 6.0 under optimal conditions, decreasing lower only under stress, e.g. under low CO_2 [5]. To maintain sufficient driving force for ATP synthesis, it was hypothesized that light-driven trans-thylakoid $\Delta\psi$ constituted a substantial portion of *pmf*. Later *in vitro* and *in vivo* measurements of the light-driven electrochromic shift (ECS) confirmed contributions of about 50% $\Delta\psi$ to *pmf*, at least under the experimental conditions used in these studies [9,10].

Establishing quantitative relationships among light-driven electron and proton transfer, the resulting *pmf*, lumen pH and regulation of light capture is essential for understanding the plants responses to environmental changes. In this work, we attempt to address these issues by estimating total *pmf* and lumen pH *in vivo* from ECS and complementary measurements.

2. Materials and methods

2.1. Plant materials

Arabidopsis thaliana (ecotype Columbia) wild type (Wt) and *npq2* [11] were grown either in a green house (~25 °C, maximum light intensity 600 μmol photons m^{-2} s^{-1}) or growth chamber (23 °C, light intensity 130 μmol photons m^{-2} s^{-1}). Three- to 4-week-old plants were dark-adapted and acclimated to room temperature (23 °C) overnight before measurements. During assays, detached leaves with petioles dipped in water were placed in the spectrophotometer leaf chamber under flowing ambient air (~372 ppm CO_2, 21% O_2), low CO_2 air (50 ppm CO_2, 21% O_2), or CO_2-free air (0 ppm CO_2, 21% O_2). To avoid dehydration, flowing air was humidified by bubbling in distilled water.

2.2. Spectroscopic measurement of electrochromic shift

Spectroscopic assays were performed using a custom-made spectrophotometer, based on those described previously [10,12]. The pulsed measuring beam for absorbance measurements consisted of green light-emitting diodes filtered through interference filters. The pulsed measuring beam for fluorescence measurements was a 535-nm light-emitting diode, with fluorescence being detected at >720 nm from the side of the leaf illuminated by the actinic and measuring lights. These wavelength ranges were chosen to allow even sampling of fluorescence responses from different layers of the leaf since green and infrared light passes relatively unobstructed through the leaf. Key measurements were repeated on a modified instrument in which the fluorescence was detected from the opposite side. Essentially identical responses comparing ECS and fluorescence signals were found, indicating that differential sampling from different leaf depths did not interfere with our measurements.

All ECS signals were normalized to the rapid (microseconds) rise in 520 nm absorbance upon a saturating, single-turnover xenon flash, independently measured on dark-adapted leaves [13,14]. This normalization accounted for changes in leaf thickness and chloroplast density between leaves which varied by about 5%, e.g. between Wt and *npq2*. We also used the flash-induced ECS to test whether illumination caused large scale changes in the optical pathlengths of the leaves, e.g. by chloroplast movements. Neither red nor blue light caused significant changes in the extent of flash-induced ECS changes as long as the illumination was not intense enough to cause photodamage (data not shown), leading us to conclude that illumination did not induce significant changes in the optical properties of the leaves.

Dark interval relaxation kinetics (DIRK) of ECS was measured during steady-state photosynthetic conditions, after 15 min actinic illumination by red LEDs (650 nm) at intensity from 55 to 794 μmol photon m^{-2} s^{-1}. The total rapid change in ECS, termed ECS_t, was measured as the absorbance change at 520 nm (ΔA_{520}) during brief (320 ms) dark intervals. For measuring ΔpH proportion in *pmf* (θ), the 'inverted' ECS signal at 520 nm, termed ECS_{inv}, during 1 min dark-interval was deconvoluted using a base line between 505 and 535 nm as described in [12,14].

2.3. Chlorophyll fluorescence measurements

The extents of LEF and q_E were calculated from saturation pulse-induced chlorophyll fluorescence yields. Chlorophyll fluorescence was excited by weak pulses of 520 nm light and fluorescence emission was detected in the near infrared region (>720 nm). LEF was calculated from quantum efficiency of PSII (Φ_{PSII}) [15,16], photosynthetically active radiation (i) and fractional capturing of photon by PSII (approximated to 0.5) [17]; LEF=Φ_{PSII}*i*0.5. q_E was calculated from a maximum fluorescence yield after 15 min actinic illumination (F'_M) and its recovery after 10 min dark period (F''_M) as in [10,14]; $q_E=F''_M/F'_M-1$. The estimates of excitation quenching derived in this way and under the present conditions were proportional to changes in absorbance at 535 nm, and thus attributable to q_E [18].

2.4. Spectroscopic measurement of cytochrome f reduction

Cyt *f* reduction was measured from ΔA_{554} after subtracting a baseline between ΔA_{545} and ΔA_{563} as described previously [7,19]. Steady-state oxidation–reduction rates were estimated by DIRK analysis as in [19]. After 10 to 15 min actinic illumination, ΔA_{554}, ΔA_{545} and ΔA_{563} measurements during 500 ms dark-interval were averaged 16 to 30 times, with 5 s actinic intervals separating each collected trace. Measurements of cyt *f* reduction were made on both green house and growth chamber grown plants, with essentially superimposable results. However, data from growth chamber grown plants gave better signal-to-noise ratios and thus are shown here.

2.5. Spectroscopic measurement of xanthophyll conversion

Deepoxidation of xanthophyll was estimated from ΔA_{505} using ΔA_{535} as a reference, after an appropriate dark time (10 min.) to allow for relaxation of q_E, as described earlier [20,21]. The ΔA_{505} was measured over a 10-min actinic illumination period (reaching steady-state) followed by a 1-min dark relaxation to distinguish xanthophyll conversion from ECS and light scattering changes (deepoxidized xanthophylls remains for tens of minutes in the dark [22]). Relatively large noise caused by chloroplast movement during illumination was mostly eliminated by using ΔA_{535} as a reference.

2.6. Data analysis and computer simulation of a kinetic model

Experimental data were plotted and fitted by the model equations (see Discussion) using Origin 6.0. Computer simulations of xanthophyll conversion were performed by a program written in-house using Microsoft Visual Basic 6.0.

3. Results

3.1. Response of the dark interval relaxation kinetics of electrochromic shift to changing CO_2 levels and light intensity

The relative changes in steady-state light-induced *pmf* and lumen pH *in vivo* were measured spectroscopically using dark interval relaxation kinetics (DIRK) analysis of ECS as discussed in detail in [4,23] and briefly as follows. The ECS signal measured at around 520 nm has been shown to respond linearly

to changes in transthylakoid $\Delta\psi$ [24], making it a useful probe of the electrogenic reactions of photosynthesis, including transmembrane proton flux through the ATP synthase. To probe *pmf*, we start from steady-state conditions, where proton influx into the lumen is precisely balanced by efflux, thus simplifying the analyses. The actinic light is then switched off for ~2 min intervals, inhibiting the proton influx associated with the light reactions while allowing proton efflux to continue. The relaxation kinetics of the ECS during the dark interval (see Fig. 1A inset) are analyzed to yield estimates of *pmf* components [9,10,25]. Light-induced *pmf* (*pmf* in light minus *pmf* in dark, $pmf_{l\text{-}d}$, *pmf* in light minus that in dark) should be proportional to total amplitude of ECS or ECS_t, the rapid (tens of ms) light–dark change in ECS. The light-induced ΔpH ($\Delta pH_{l\text{-}d}$) should be proportional to inverted ECS or ECS_{inv}, the slowly-reversible (tens of s) phase of ECS decay. The difference between ECS_t and ECS_{inv} should reflect the $\Delta\psi$ portion of light-induced *pmf* ($\Delta\psi$ in light minus $\Delta\psi$ in dark, $\Delta\psi_{l\text{-}d}$).

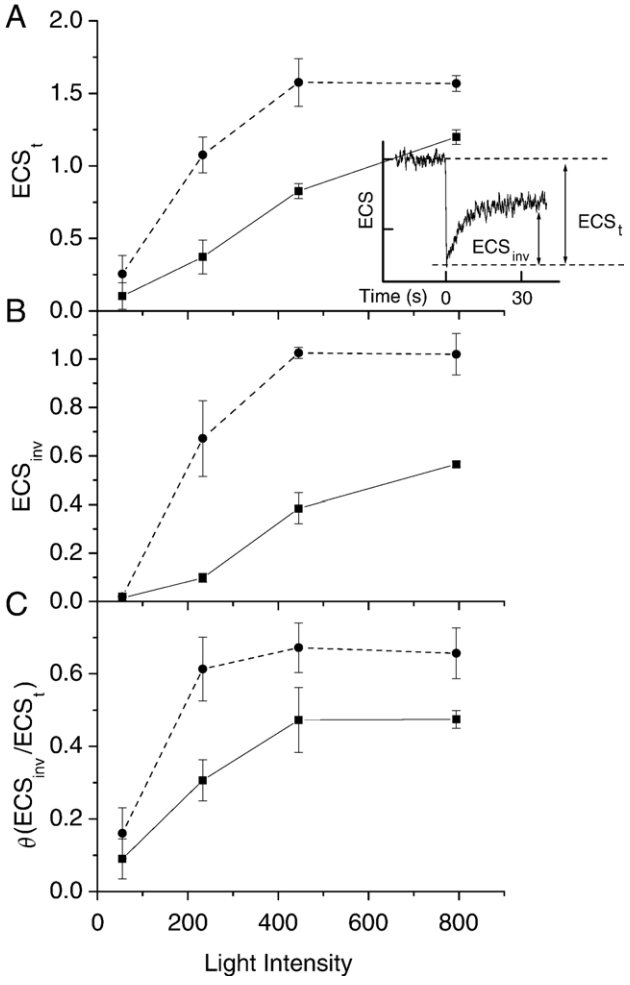

Fig. 1. Response of ECS parameters to changing CO_2 levels and light intensity. ECS_t (Panel A), ECS_{inv} (Panel B), and θ, ECS_{inv}/ECS_t (Panel C) were measured in Wt leaves at a range of steady-state light intensities, 55, 233, 445, 794 μmol photons m^{-2} s^{-1} under ambient air (■, $n=4\pm$se) and 50 ppm CO_2 (●, $n=4\pm$se). ECS parameters were normalized by a saturation pulse-induced potential rise for compensating a difference in the reaction center density. Panel A inset shows typical ECS measurement sequence after light-to-dark transition. Actinic illumination was turned of at time 0. The amplitude of ECS drop at time 0 is ECS_t and the subsequent recovery phase is ECS_{inv}.

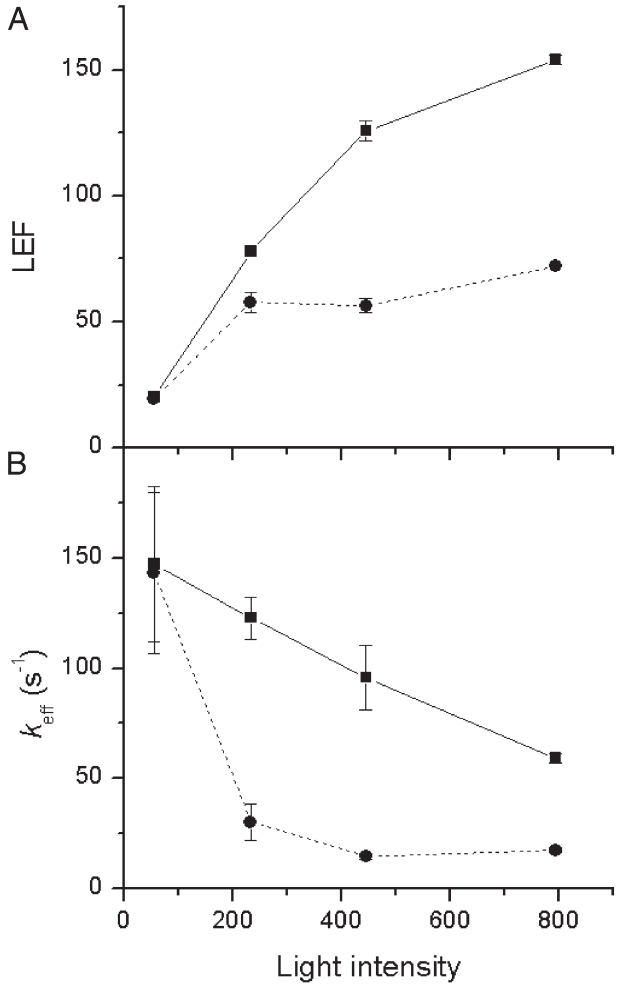

Fig. 2. Response of the LEF and cyt *f* reduction to changing CO_2 levels and light intensity. LEF (Panel A) and effective rate constant (k_{eff}) of cyt *f* reduction (Panel B) were measured in Wt leaves at a range of steady-state light intensities, 55, 233, 445, 794 μmol photons m^{-2} s^{-1} under ambient air (■, $n=4\pm$se) and 50 ppm CO_2 (●, $n=4\pm$se).

ECS parameters (normalized as described in Materials and Methods) were measured under steady-state illuminated conditions in leaves of *Arabidopsis* wild type (Wt). Under ambient CO_2 (~372 ppm) and O_2 (21%), ECS_t increased with increasing light intensity from 55 to 794 μmol photons m^{-2} s^{-1} (Fig. 1A). Lowering CO_2 to 50 ppm (maintaining O_2 at 21%) enhanced the response of ECS_t to light intensity, an effect predominantly attributable to a decrease in the proton conductivity of the ATP synthase (data not shown), as previously observed in tobacco [10,26] and in *Arabidopsis* [14].

Responses of ECS_{inv}, reflecting the ΔpH component of *pmf*, were qualitatively similar to those of ECS_t but with higher sensitivity at low CO_2 (Fig. 1B). The fraction of *pmf* stored as ΔpH, a parameter we term θ, estimated by ECS_{inv}/ECS_t, changed from 0.1 to 0.5 as the light intensity increased to saturation (Fig. 1C). A similar effect was previously observed in *Arabidopsis* [14] and in intact tobacco plants [10] when both CO_2 and O_2 were lowered and attributed to a regulatory

response, where increases in θ result in more sensitive q_E responses.

3.2. Response of the effective rate constant for plastoquinol oxidation at cyt b_6f complex to changing CO_2 levels and light intensity

Fig. 2A shows the light response of linear electron flow (LEF) in Wt leaves, estimated using saturation pulse-induced chlorophyll fluorescence changes (see [15,17]). At 372 ppm CO_2 and 20% O_2, LEF was half-saturated at ~300 μmol photons m^{-2} s^{-1} and reached a maximal rate of ~130 μmol electrons m^{-2} s^{-1}. Decreasing the CO_2 levels to 50 ppm caused a decrease in the maximal LEF rate to ~70 μmol electrons m^{-2} s^{-1} and in the half-saturating light intensity to ~120 μmol photons m^{-2} s^{-1}.

Fig. 2B shows the effective rate constant (k_{eff}) for plastoquinol oxidation monitored by cyt *f* reduction upon rapid light–dark transitions from steady-state illumination (see Materials and methods and [6,7,19]). (We note that k_{eff} cannot, by itself, be directly compared to LEF; estimates of flux using cyt *f* kinetics would require consideration of the extent of cyt *f* oxidation as well as electron sharing between cyt *f*, plastocyanin and P_{700} [19]). Under 372 ppm CO_2 and 20% O_2, k_{eff} slowed from 147 to 59 s^{-1} from low to saturating light. When the CO_2 was lowered to 50 ppm, cyt *f* k_{eff} ranged from ~45 to ~15 s^{-1}, reflecting increased restriction in plastoquinol oxidation upon lumen acidification, as observed previously [27]. In contrast, in tobacco, cyt *f* reduction remained constant from low to saturating light decreasing only upon lowering CO_2 levels (reviewed in [5]).

3.3. Response of the q_E to changing CO_2 levels and light intensity

In vivo activation of q_E and its two lumen pH-dependent components, xanthophyll cycle conversion and protonation of PsbS, were estimated in *Arabidopsis* Wt and *npq2*, which continuously accumulates deepoxidized xanthophyll [11]. As measured from chlorophyll fluorescence, q_E was always proportional to absorbance changes at 535 nm (data not shown), in accord with the previously reported strict interdependence of these two signals [28,29]. Parameters were measured under a range of light intensities and under ambient CO_2, 50 ppm CO_2 or CO_2-free air.

In Wt under ambient air (Fig. 3A), q_E increased sigmoidally with a distinct, insensitive phase at low light intensity. In earlier work (e.g. [22]), this lag phase was likely obscured by contributions from other NPQ processes, mostly photoinhibitory quenching or q_I [30]. Lowering the CO_2 level to 50 or 0 ppm dramatically increased the q_E response to light intensity, as previously observed [26]. In contrast to Wt, *npq2* did not show an initial lag (insensitive) phase in q_E response to light intensity (Fig. 3B, cf. Fig. 6 in ref. [11]). Light saturation curves of LEF were indistinguishable between Wt and *npq2* (data not shown).

Fig. 3C shows the extents of steady-state light-induced deepoxidation of xanthophylls in Wt leaves, estimated by ΔA_{505}

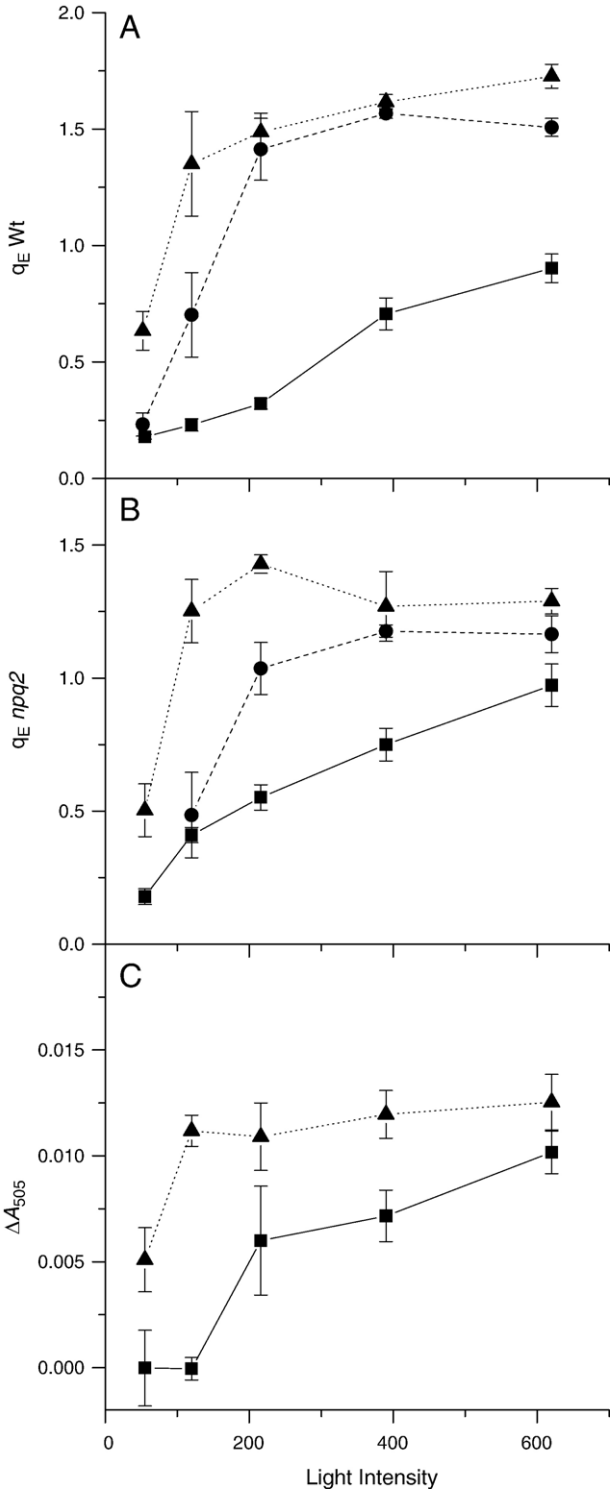

Fig. 3. Response of q_E to changing CO_2 levels and light intensity. q_E and ΔA_{505} were measured under varied steady-state illumination, 55, 120, 216, 390, 620 μmol photons m^{-2} s^{-1}, and CO_2 level. Panel A: q_E was measured in Wt leaves under ambient air (■, $n=6\pm$se), 50 ppm CO_2 (●, $n=3\pm$se), and CO_2-free air (▲, $n=5\pm$se). Panel B: q_E in *npq2* was measured under ambient air (■, $n=8\pm$se), 50 ppm CO_2 (●, $n=4\pm$se), and CO_2-free air (▲, $n=4\pm$se). Panel C: ΔA_{505} in Wt leaves was measured under ambient air (■, $n=6\pm$se) CO_2-free air (▲, $n=5\pm$se).

[20–22]. With 372 ppm CO_2, 20% O_2, the light saturation curve of ΔA_{505} was sharply sigmoidal, with a lag phase at light intensities below about 120 μmol photons m^{-2} s^{-1}. Upon lowering CO_2 to 50 ppm, the response of ΔA_{505} became more sensitive to light intensity. No ΔA_{505} signals attributable to q_E were observed in *npq2* (data not shown), as expected from previous work [11], showing that xanthophyll is maintained in its deepoxidized state in this mutant.

4. Discussion

4.1. Investigations intrinsic pH-dependent processes by ECS_{inv}

In this section, we explore the relationships between various lumen pH-dependent processes and our (at this point qualitative) estimate of light-induced ΔpH (ECS_{inv}). Fig. 4A–D show the dependences of four processes on ECS_{inv} (proportional to the ΔpH component of *pmf*), 1) the logarithm of effective rate constant for cyt *f* reduction, reflecting the pH-dependence of plastoquinol oxidation at the cyt b_6f complex (Fig. 4A); 2) the conversion of violaxanthin (V) to zeaxanthin (Z) via antheraxanthin (A) measured by the ΔA_{505} change, reflecting the pH-dependent activation of V deepoxidase (VDE) (Fig. 4B); 3) q_E in *npq*2, reflecting changes in lumen pH when Z is saturated, most likely reflecting PsbS protonation (Fig. 4C); and 4) q_E in Wt, reflecting both VDE activation and (likely) PsbS protonation (Fig. 4D). The data were fit, rather arbitrarily at this point (but see below), to Hill equations. The noise level largely reflects the difficulty in measuring ECS_{inv}, which requires deconvolution of ECS signal using three separate wavelengths over extended periods (many seconds).

Even without calibration of the signals, these data allow us to make some important conclusions about the nature and roles of the thylakoid *pmf*. Most strikingly, the responses appear to be continuous (smooth) functions of estimated light-induced ΔpH, despite the fact that the ΔpH was varied both by changing light intensity and CO_2 levels. In other words, no apparent deviations were observed that might indicate that these processes 'feel' different extents of ΔpH, as one would expect for altering their modes of action or switching between localized versus delocalized proton gradients [20] since such processes should have yielded strongly scattered or discontinuous relationships in Fig. 4.

The differences in the dependencies of Z accumulation and PsbS protonation are also striking. These responses arise from differences in the cooperativity (Hill coefficient or n_H) for protonation of VDE and PsbS, the former being reported as around 5 [31] and the latter probably being 1 or 2 (see below). The response of q_E lies somewhere between that of Z accumulation and PsbS protonation, supportive of models where both processes are required for activation of q_E [32] (see also below).

4.2. Quantitative estimates of *pmf*

As discussed previously [4,23,33], calibrating the ECS response should allow us to make quantitative estimates of *pmf*, Δψ and ΔpH. Since the ECS signal is a linear indicator of Δψ, we need only to determine the slope of the relationship

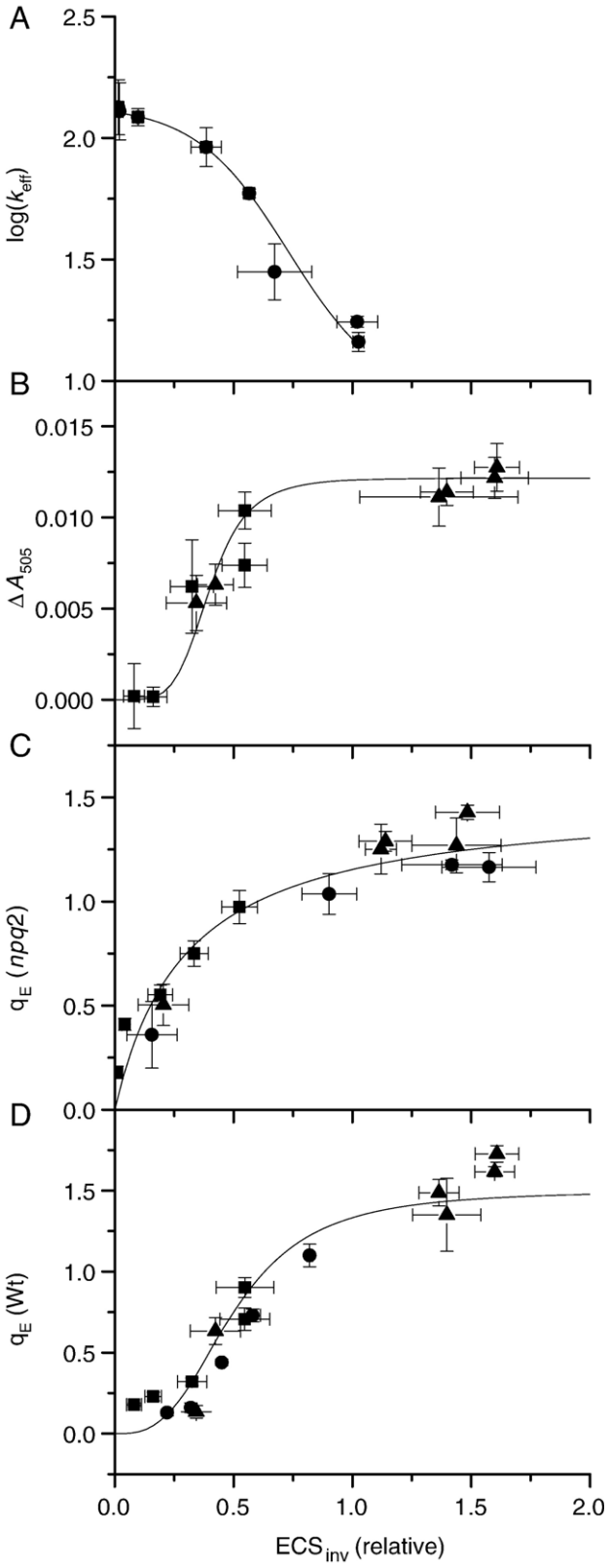

Fig. 4. The profile of pH dependent reactions plotted as a function of ECS_{inv}, used as an approximate indicator of change in lumen pH. Logarithm of k_{eff} (Panel A), ΔA_{505} (Panel B), q_E in *npq2* (Panel C) and Wt (Panel D) measured as Figs. 2B, 3C, B and A respectively were plotted against simultaneously measured ECS_{inv}. The logarithm of k_{eff} was plotted in Panel A because these values should be proportional to lumen pH below the effective pK_a for PQH_2 oxidation.

between ECS and $\Delta\psi$, a factor we term C, which should be possible by comparing ECS to intrinsic lumen pH-dependent signals. The calibrating signals do not need to be linear indicators of lumen pH, but at least must exhibit reproducible transitions that follow defined pH-responses. Here we used n_H and the pK_a of plastoquinol oxidation at cyt b_6f complex as primary constraints, since their behavior has been well characterized *in vitro*, and follow this up by several external validity checks (see below).

One complication is that calculating pH in thylakoid lumen (pH_{lumen}) also requires estimates of dark-sustained *pmf* (pmf_d) and stromal pH (pH_{stroma}). However, previous observations give us estimates of pmf_d and pH_{stroma} within relatively small ranges (as discussed below). We conclude that the pmf_d and pH_{stroma} are relatively constant under our experimental conditions since substantial changes in these parameters should measurably alter the relationships between ECS_{inv} and q_E, which previously have not been observed (see [10,26]).

The relationships between light-induced *pmf* ($pmf_{l\text{-}d}$), light-induced $\Delta\psi$ ($\Delta\psi_{l\text{-}d}$) and light-induced ΔpH ($\Delta pH_{l\text{-}d}$) and the corresponding ESC parameters can be written in the following simple equations:

$$pmf_{l\text{-}d} = C \cdot ECS_t, \tag{1a}$$

$$\Delta\psi_{l\text{-}d} = C \cdot ECS_{ss}, \tag{1b}$$

and

$$\Delta pH_{l\text{-}d} = \frac{F}{2.3RT} \cdot C \cdot ECS_{inv} \approx \frac{1}{59\ mV} \cdot C \cdot ECS_{inv}. \tag{1c}$$

It is important to note that *pmf* is maintained across the thylakoid membrane *in vivo* even in the dark and that the signals we measure will reflect *pmf* components offset by values reflecting 'dark' *pmf* or pmf_d [9,13,34,35]. In vascular plants, pmf_d is probably the result of ATP hydrolysis at the ATP synthase, but substantial contributions from 'chlororespiration' or related processes are seen in algae [35,36]. In our experiments on vascular plants [10,14,26], the decay of the ECS during short dark interval in light-adapted leaves was mono-exponential, reflecting an apparent single pseudo-first order process, indicating that under these conditions pmf_d is sufficient to maintain the ATP synthase in an active state when its γ-subunit is in its reduced form. Thus, at least in light-adapted leaves we expect pmf_d to come into equilibrium with ΔG_{ATP} during dark intervals [9,26] and remain so over the tens of minutes required to oxidize the ATP synthase γ-subunit [13]. ΔG_{ATP} measured in the dark and the light is estimated to range between 40 and 50 kJ/mol [37,38], corresponding to 90–112 mV in pmf_d, assuming that the proton ATP ratio is 4.67 [39]; the upper estimate of 112 mV agrees well with other independent *in vitro* measurements of threshold *pmf* required to maintain the ATP synthase in its active state [1,40].

The total *pmf* under steady-state illumination (pmf_{ss}) will be the sum of pmf_d (dark-stable component, in equilibrium with ΔG_{ATP}) and $pmf_{l\text{-}d}$ (light-induced component, which is out of equilibrium with ΔG_{ATP} because of the substantial light-driven proton flux),

$$pmf_{ss} = pmf_{l\text{-}d} + pmf_d. \tag{2}$$

Combining with Eq. (1a) yields,

$$pmf_{ss} \approx C \cdot ECS_t + pmf_d. \tag{3}$$

We next assess the lumen pH imposed by *pmf*. In earlier work, (see [9,10]) we showed that θ (the fraction of *pmf* stored as ΔpH) for light-induced *pmf* can be estimated by ECS_{inv}/ECS_t. Here we assume that the same θ can be applied to both light-induced and dark *pmf*. This should be true as long as the proton buffering capacity of the lumen is reasonably constant over the pH range experienced by the lumen (see discussion in [9,41]). The estimated ΔpH under steady-state illumination, termed ΔpH_{ss}, can thus be expressed as,

$$\frac{2.3RT}{F}\Delta pH_{ss} = \theta \cdot pmf_{ss}, \tag{4}$$

And at room temperature,

$$\Delta pH_{ss} \approx \frac{1}{59\ mV} \cdot \theta \cdot (C \cdot ECS_t + pmf_d). \tag{5}$$

The lumen pH (pH_{lumen}) in the light can thus be estimated as

$$pH_{lumen} = pH_{stroma} - \Delta pH_{ss} \approx pH_{stroma} - \frac{1}{59\ mV} \cdot \theta \cdot (C \cdot ECS_t + pmf_d). \tag{6}$$

4.3. The oxidation of plastoquinol by the cyt b_6f complex

It is well known that the kinetics of plastoquinol oxidation at the Q_o site of the cyt b_6f complex are pH-dependent [6,7]. Here, we used the inverse of the lifetime for cyt *f* reduction, as a phenomenological (or empirical) indicator of the k_{eff} for plastoquinol oxidation [7]. The logarithm of the k_{eff} is observed to be proportional to pH below its apparent pK_a, as follows

$$\frac{k_{eff}}{k_{eff\ MAX}} = \frac{1}{10^{n_H \cdot (pK_a - pH_{lumen})} + 1}, \tag{7a}$$

and

$$\log(k_{eff}) = \log(k_{eff\ MAX}) - \log(10^{n_H \cdot (pK_a - pH_{stroma} + \Delta pH_{ss})} + 1) \tag{7b}$$

where $k_{eff\ MAX}$ is the maximum value of the k_{eff} (above the pK_a) and n_H and pK_a are the apparent Hill coefficient and pK_a for plastoquinol oxidation. Experiments on uncoupled thylakoids [7] and isolated cyt b_6f complexes [6] showed an apparent pK_a of ~6.1 and n_H of ~1.2. The physical basis of the observed $n_H > 1$ is unclear (see [6]) but probably reflects protonation of multiple residues on the b_6f complex.

Fig. 5 shows a plot of the data in Fig. 4A, but with the 'upper' *x*-axis set to estimated 'ΔpH' using Eq. (5). The calculation of ΔpH from the ECS_{inv} data in Fig. 4A takes into consideration the partitioning of total *pmf* into $\Delta\psi$ and ΔpH, thus resulting in

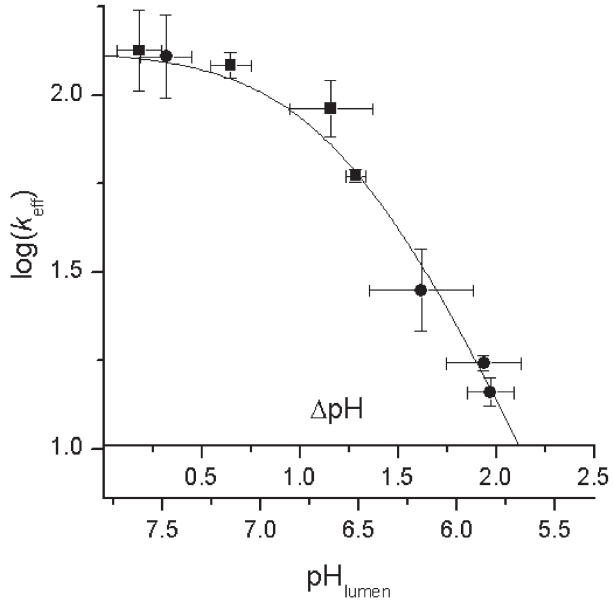

Fig. 5. Data plotting against estimated lumen pH and fitting a model equation. The logarithm of k_{eff}, measured as Fig. 2B, was plotted against calculated ΔpH estimated by Eq. (5) (upper scale on the *x*-axis) and pH_{lumen} estimated by Eq. (6) (lower scale on the *x*-axis). The values of pmf_d and pH_{stroma} were assumed to be 112 mV, and 7.8, respectively. The Hill coefficient, n_H, and pK_a for PQH_2 oxidation at the cyt b_6f complex were taken to be 1.2 and 6.6, respectively. The best-fit curve (R^2=0.979) yielded C=40 mV/ECS-unit.

small changes in the overall shape of the response. The data remained a continuous function of calculated ΔpH. A best-fit curve to the data in Fig. 5 using n_H=1.2 and pmf_d=112 mV yielded C=40 mV/ECS-unit. This is well within the range of reasonable estimates of C, obtained from the physical properties of thylakoid membranes. For example, assuming a density of PSI+PSII reaction centers of 4×10^{-13} mol cm^{-2} [42] and specific capacitance of the thylakoid membrane of 1 μF cm^{-2} [43], one estimates a flash-induced transthylakoid potential of 38 mV (see also [9]).

In general, estimated values for C increased when we assumed smaller n_H and pmf_d values. For example, decreasing n_H from 1.2 to 1.0 (with constant pmf_d at 112 mV), increased C from 40 to 50 mV/ECS-unit, but resulted in slightly worse fitting to the model equation; the R^2 value calculated for the least squares regression decreased from 0.979 to 0.976. Decreasing the assumed value of pmf_d from 112 to 90 mV (with n_H=1.2) increased the estimated value of C from 40 to 55 mV/ECS-unit, but decreased R^2 from 0.979 to 0.968. The fact that the changes in R^2 were small indicates that a range of values for C are acceptable, but C=40 mV/ECS-unit (with pmf_d=112 mV) was the most favorable and, as seen below, consistent with the overall responses of a range of lumen pH probes. Moreover, making changes in C of this order had only small effects on the estimates for lumen pH or on our overall conclusions.

Assuming C=40 and pmf_d=112 (see above) we arrive at a pK_a for cyt *f* reduction of approximately 1.2 pH units below the assumed pH_{stroma}. With pH_{stroma}=7.8 [44–46] we obtain an apparent pK_a for cyt *f* reduction of 6.6 (see Fig. 5, *x*-axis labeled 'pH_{lumen}'), close to *in vitro* estimates of pK_a 6.1–6.5 (see above).

4.4. In vivo analysis of q_E activation

Light-induced deepoxidation of V to A and Z by VDE [47] is involved in activation of q_E quenching [48,49]. VDE is localized in thylakoid lumen and its activity is highly dependent on lumen pH [50]. The apparent n_H and pK_a values for VDE protonation have been estimated *in vitro* to be 4.5±0.5 and 6.25±0.25 respectively [31,51–54].

The steady-state accumulation of Z and A (Z+A) should obviously depend on the activation status of VDE, which responds to lumen pH. What is not so obvious is that the quantitative relationship between lumen pH and Z+A accumulation should also depend on the activity of Z epoxidase (ZE), which mediates the reverse reaction from Z to V via A [50]. ZE is located on the stromal side of the thylakoid and thus its activity should be independent of lumen pH [50] but should nevertheless influence the steady-state accumulation of Z+A. To illustrate, consider the case where ZE activity is near zero, in which Z+A will accumulate to large extent even with little VDE activation, as is the case with *npq2* [11,55]. In contrast, with a large ZE activity, a higher VDE activation state will be needed to accumulate the same amount of Z+A, simply because ZE will rapidly reconvert Z and A back to V. It follows that the apparent pK_a for Z+A accumulation will be shifted from that for VDE activation by a factor related to the ratio of ZE activity to maximal VDE activities. The lower ZE activity is with respect to maximal VDE activity, the less acidic the lumen needs to be to achieve a certain Z+A accumulation. Results from *in vitro* experiments [21,31,56,57] suggest that maximal light-induced turnover rates for VDE are substantially (roughly 20 to 300 times) faster than those for ZE , which should shift the *apparent* pK_a towards higher pH values.

Kinetic simulations (Fig. 6), assuming a n_H of 4 and a pK_a of 6 for VDE activation (see solid line in Fig. 6), predict that the effective pK_a for Z+A accumulation will increase from 6 to 6.7 as the ratio of maximal VDE/ZE rate increases from 1 to 300. Despite these differences, the relationships can still be fit *empirically* to the Hill equation, albeit with altered parameters. The following equation can be used to describe the simulated steady-state xanthophyll status, reflecting the *effective* values of pK_a (pK_{a1}) and n_H (n_{H1}),

$$\frac{\Delta A_{505}}{\Delta A_{505\ MAX}} = \frac{[Z+A]}{[V+A+Z]} = \frac{1}{10^{n_{H_1}\cdot(pH_{lumen}-pK_{a_1})}+1} \quad (8)$$

where ΔA_{505MAX} is the maximum absorption change at 505 nm.

Protonation of the PsbS protein is also required for initiation of q_E quenching [18,58] and thus should reflect lumen pH. In the *Arabidopsis npq2* mutant [11], which constitutively accumulates Z, q_E is limited only by protonation of PsbS protein and should obey the Hill relationship,

$$\frac{q_{E,\ npq2}}{q_{E,\ npq2\ MAX}} = \frac{[PsbS\cdot H^+n]}{[PsbS]+[PsbS\cdot H^+n]} = \frac{1}{10^{n_{H2}\cdot(pH_{lumen}-pK_{a2})}+1}. \quad (9)$$

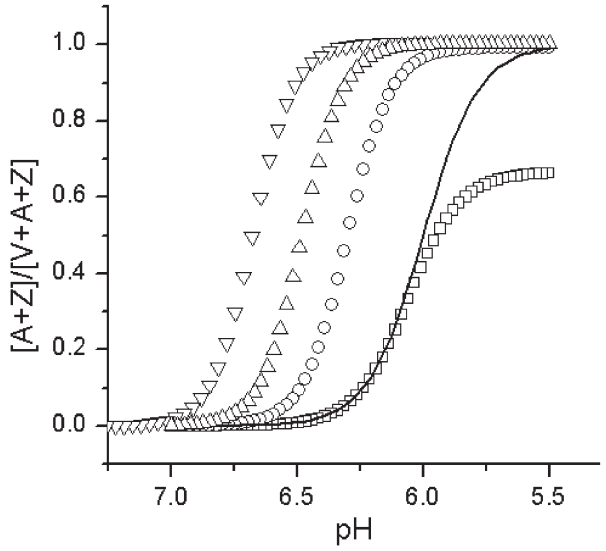

Fig. 6. Kinetic simulations of Z+A accumulation. pH dependency of steady-state Z+A accumulation was simulated under different maximum activity of VDE comparing to ZE as described in the text, with the maximal rates of VDE/ZE=1 (□), 10 (○), 50 (△), 300 (▽), whose effective pK_a were 6.1, 6.3, 6.5, 6.7, respectively. A solid line shows pH-dependent VDE activation curve (n_H=4 and pK_a=6) used for the simulations.

where $q_{E,npq2MAX}$ is the maximal q_E in *npq2* mutant observed under saturating lumen acidity (where PsbS is fully protonated). PsbS and PsbS·H^+_n are the deprotonated and protonated forms of PsbS; pK_{a2} and n_{H2} are the effective values of pK_a and n_H for PsbS protonation. Since protonation of two Glu residues of PsbS protein are involved in the q_E response [29], n_{H1} will probably be between one and two, depending upon whether the protonation of the two residues is cooperative. Site-directed mutants lacking one of the two Glu residues on PsbS showed diminished q_E, but the half-time for onset of q_E was essentially identical to those of Wt [29], suggesting that each Glu residue acts additively but non-cooperatively, and thus we suggest that n_{H1} is unity.

In current models for antenna regulation, the extent of q_E is controlled by both Z+A accumulation and PsbS protonation [2,29,59], as diagramed in Fig. 7. A straightforward formulation of this model, where the extent of q_E is dependent on the product of Z+A accumulation and PsbS protonation, can be expressed as follows,

$$\frac{q_E}{q_{E\ MAX}} = \frac{[Z+A]}{[V+A+Z]} \cdot \frac{[\mathrm{PsbS}\cdot \mathrm{H}^+ n]}{[\mathrm{PsbS}]+[\mathrm{PsbS}\cdot \mathrm{H}^+ n]} = \frac{1}{10^{n_{H1}\cdot(\mathrm{pH}_{lumen}-\mathrm{p}K_{a1})}+1} \cdot \frac{1}{10^{n_{H2}\cdot(\mathrm{pH}_{lumen}-\mathrm{p}K_{a2})}+1} \quad (10)$$

where the n_H and pK_a parameters are the effective protonation parameters for PsbS protonation and Z+A accumulation, as described above. Implicit in Eq. (10) is a linear response of q_E with [Z+A] at a constant PsbS protonation, as shown by Gilmore et al. [59]. This nonsaturating response implies that either multiple Z and A molecules can associate with a given antenna or that the association is weak.

Fig. 8A–C show Z+A accumulation (ΔA_{505}), PsbS protonation (q_E in *npq2*) and q_E plotted against lumen pH estimated by our calibrated ECS assay. Using C=40 mV/ECS-unit, pmf_d=112 mV and pH stroma=7.8 yielded good agreement with the model (using Eqs. (8), (9) and (10) for Z+A, PsbS protonation and q_E gave R^2=0.975, 0.911 and 0.936 respectively). Z+A accumulation and PsbS protonation predicted very similar effective pK_a values (~6.8), but very different n_H values (~4.3 vs. ~1.0 respectively). These fits conform to the expected relative Hill coefficients for the two processes [31,51–53], partially validating our estimates.

The pK_a of protonation of VDE determined *in vitro* is between 6.0 and 6.5 [31,51–53]. The apparent pK_a for Z+A accumulation from our fit to Fig. 8A is shifted upwards from *in vitro* estimates by 0.3 to 0.8 units. Within the context of the model presented in Fig. 6, this shift implies that the maximal ZE turnover rate is between 10 and 300 times slower than that of VDE, consistent with published data [21,57]. These results indicate that the chloroplast might adjust the pH range of the xanthophyll cycle responses by regulating ZE activity. In this context, it is interesting to note that VDE and ZE could be differentially regulated during stress or development, suggesting that the responses of Z+A accumulaton to lumen pH might be adjusted as an acclimatization response [60–63].

4.5. Quantitative estimates of lumen pH in vivo

Fig. 9A shows estimates of total steady-state *pmf* (termed pmf_{ss}) using Eq. (3) with C=40 mV/ECS unit, pmf_d=112 mV. The amplitudes of pmf_{ss} (steady-state *pmf*, ΔpH and $\Delta\psi$) ranged from 116 to 160 mV under 372 ppm CO_2, 20% O_2. At 50 ppm and 20% O_2, we estimated a maximal *pmf* of 175 mV at high light (>445 μmol photons m^{-2} s^{-1}). All *pmf* values were within the linear force-flux range for ATP synthesis at the ATP synthase [1,64].

Fig. 9B shows predicted pH_{lumen} (lumen pH under steady-state illumination), based on Eq. (6), C=40 mV/ECS unit, pmf_d=112 mV. These estimates are probably only accurate to ±0.5 pH

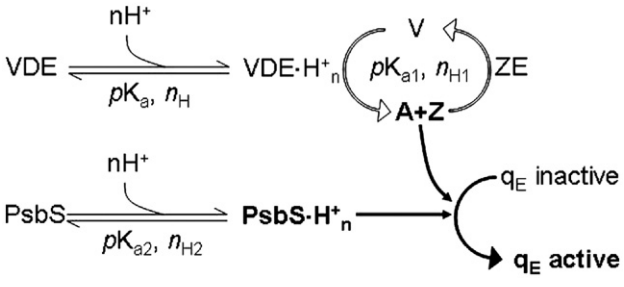

Fig. 7. q_E activation model. A working model was constructed based on our observations and those of others [2,29,59]. Conversion of light harvesting complex II from the q_E inactive to q_E active form requires both protonation of PsbS and accumulation of Z+A. These processes are regulated by pH with specific equilibrium constants (pK_a and pK_{a2}) and Hill coefficients (n_H and n_{H2}). Steady-state concentration of Z+A is determined by the relative activities of VDE to ZE, with effective pK_a (pK_{a1}) and Hill coefficient (n_{H1}) as described in Fig. 6 and the text.

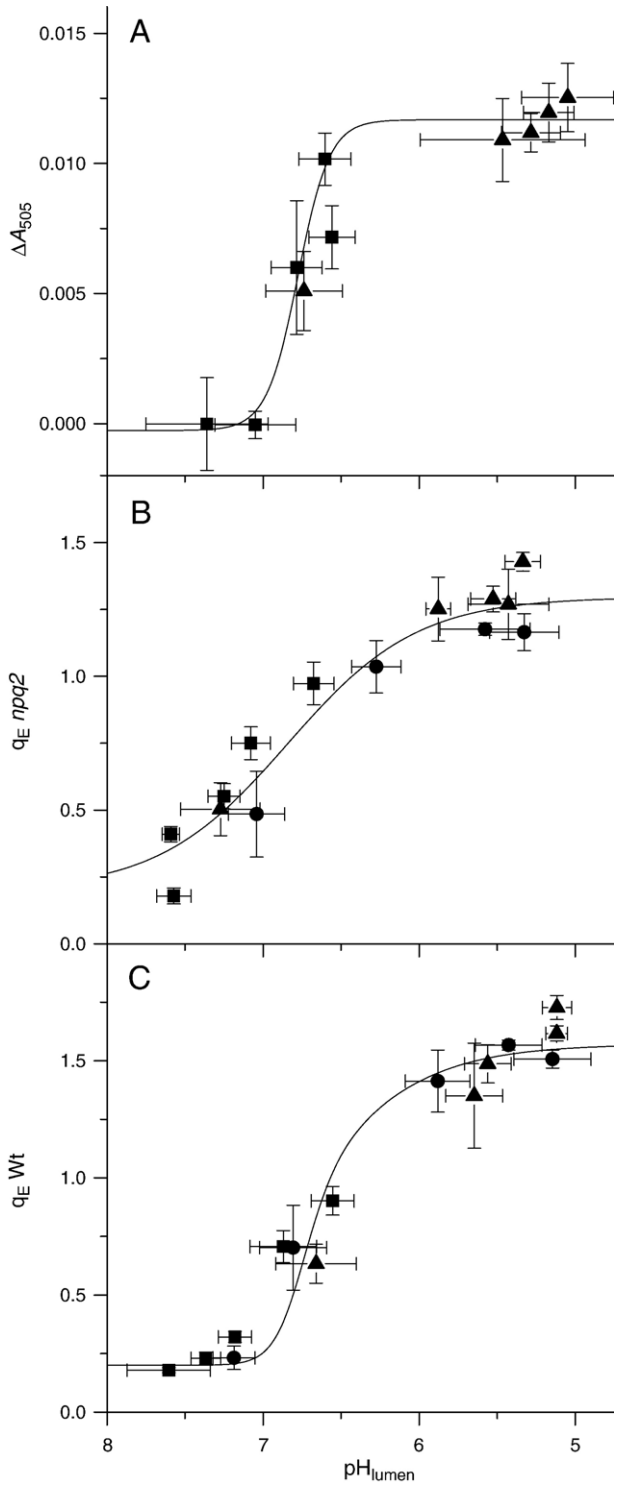

Fig. 8. *In vivo* pH response of xanthophyll cycle status, PsbS protonation and onset of q_E. Panel A, ΔA_{505} reflecting accumulation of Z+A; Panel B, protonation of PsbS as reflected by measurements of q_E in *npq2*; and Panel C, onset of q_E in Wt. Measurements were made as described in Fig. 3 and Materials and methods, and plotted against lumen pH calculated from Eq. (6) with C=40 mV/ECS-unit, pmf_d=112 mV and pH_{stroma}=7.8. Solid curves show fits to model equations; Eq. (8) for Z+A accumulation gave R^2=0.975 with n_{H1}=4.3 and pK_a=6.8, Eq. (9) for PsbS protonation gave R^2=0.911 with n_{H1}=1.0 and pK_a=6.8, Eq. (8) for q_E activation gave R^2=0.936 with n_H and pK_a values as in Z+A accumulation and PsbS protonation.

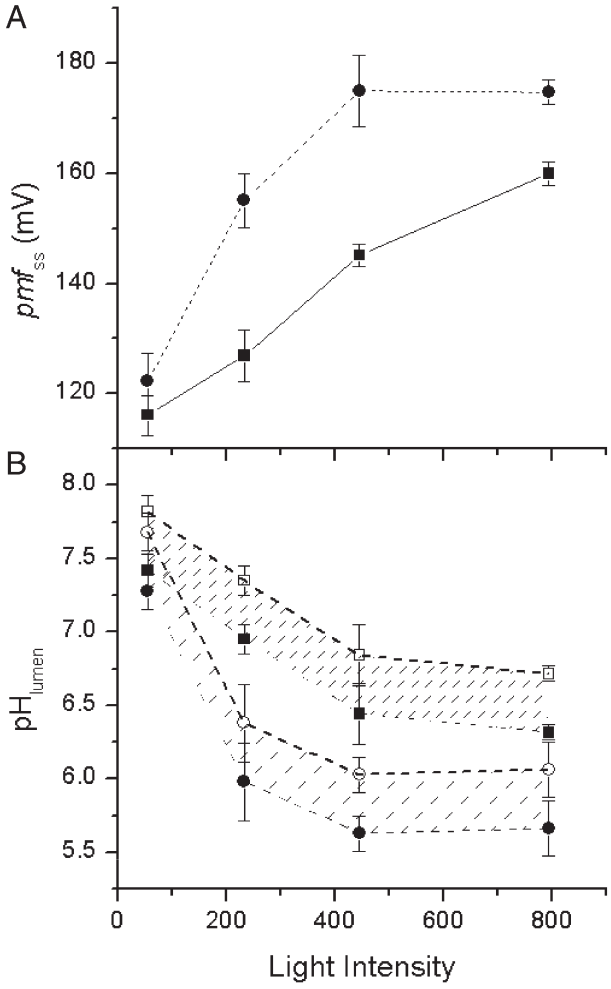

Fig. 9. Estimates of *in vivo* steady-state lumen *pmf* (pmf_{ss}) and pH. Panel A estimated *in vivo* steady-state *pmf* (pmf_{ss}); Panel B estimated lumen pH. Measurements were made under ambient air (■ and □, n=4±se) and 50 ppm CO_2 (● and ○, n=4±se). pmf_{ss} and lumen pH were calculated from Eqs. (3) and (6) using ECS parameters as in Fig. 1. C and pmf_d were assumed to be 40 mV/ECS-unit and 112 mV respectively. A range of lumen pH was calculated depending on the range of stromal pH between 7.6 (closed symbols) and 8.0 (open symbols).

units, owing mainly to ambiguities in estimates of pmf_d and pH_{stroma}. The upper and lower data sets in Fig. 9B illustrate the range with pH_{stroma} between 7.6 and 8.0 [44–46]. Under ambient air and low light, pH_{lumen} is predicted to be about 7.5. Increasing light intensity lowered pH_{lumen} to between 6.3 and 6.7, just around the apparent pK_a for plastoquinol oxidation at the cyt b_6f complex (see Fig. 5, squares). In tobacco, there is no restriction of the b_6f complex, even at high light, at unstressed plants at ambient CO_2, but plastoquinol oxidation slows when CO_2 is lowered [5,27,65]. In *Arabidopsis*, on the other hand, k_{eff} for the b_6f complex slows with increasing light intensity even at ambient CO_2 (Fig. 5, squares, see also [14]), possibly as an adaptation to growth at low light. When CO_2 was decreased to 50 ppm, estimated lumen pH decreased to as low as 5.7 to 6.1 at high light, where plastoquinol oxidation was substantially slowed (see Fig. 5, circles).

We emphasize the importance of θ, the fraction of *pmf* stored as ΔpH, in maintaining this range of pH_{lumen} in *Arabidopsis*. Our ECS assays (Fig. 1C) suggest that ΔpH constitutes a scant

10–20% of *pmf* at low light, but that this increased between 40% at high light intensity, and at 70% at both high light and low CO_2. As discussed previously [10,25], such changes in θ are critical for understanding the relationship between light-driven *pmf* and antenna regulation. How θ is regulated remains unknown, but we have suggested that alterations in stromal ion balance might differentially dissipate $\Delta\psi$, allowing ΔpH to build up to varying extents [9]. There appears to be significant species differences in θ responses. In tobacco [10,26], we previously observed constant θ values under changing CO_2 and light, but substantial changes in θ only when O_2 was lowered. *Arabidopsis* appears to have a much more sensitive control of θ, resulting in a higher range of responses to changing CO_2 and light. This makes it essential to measure θ to obtain even relative estimates of ΔpH. In addition, we speculate that the differences θ responses to physiological status represent adaptations to the plants growth light.

4.6. The regulation of electron transport by lumen pH

It has been proposed for some time that photosynthetic electron transfer can be regulated (or controlled) by lumen pH at the level of plastoquinol oxidation at the cyt b_6f complex [6,66]. This behavior could have evolved to prevent excessive reduction of PSI electron acceptors, which can lead to superoxide generation and photodamage [67]. On the other hand, slowing electron transfer at the cyt b_6f complex can lead to buildup of reduced plastoquinone and subsequently Q_A^- in PSII, also resulting in photodamage [68]. Clearly, any regulation of the cyt b_6f complex must be well balanced to prevent either type of photodamage.

Our data demonstrate that the onset of q_E occurs at a lumen pH somewhat higher than that which slows the cyt b_6f complex. Accordingly, we observe half-activation of q_E at about pH 6.5 (Fig. 8C), just where the cyt b_6f complex is *beginning* to slow (Fig. 5). Thus, we propose that the chloroplast 'tunes' the pH-response of the xanthophyll cycle with respect to that of the cyt b_6f complex to lower excitation pressure at PSII before electron transfer is slowed, preventing buildup of Q_A^-.

The pH-profile of q_E is clearly triphasic, as a result of the interplay of Z+A accumulation and PsbS protonation (Fig. 8C). We suggest that this complex response has a regulatory role. The 'lag' phase at high lumen pH allows high efficiency light capture, required for growth at low light intensity [69]. The steep increase as VDE becomes activated allows for precise transition between 'high efficiency' and 'photoprotective' modes, where substantial Q_A^- buildup must be avoided to prevent photodamage (see discussion in [70]). Finally, a gradual increase at lower lumen pH allows for fine tuning at high light/low CO_2.

Our simulations (Fig. 6) suggest a likely mechanism for 'tuning' the q_E response, involving differential expression of VDE and ZE, which will result in a shift in the apparent pK_a for Z+A accumulation. Overexpressing ZE should shift the apparent pK_a for Z+A accumulation to lower lumen pH, below that of the cyt b_6f complex kinetics. This should result in the inability to fully activate q_E (since electron transfer is slowed by low lumen pH before accumulation of Z+A) and subsequent photodamage. Indeed, Shikanai and coworkers [71] found that such effects for the complementary situation. In the *Arabidopsis* mutant *pgr*1, the cyt b_6f complex was found to be more pH-dependent, so much so that electron flow was slowed substantially before q_E was fully engaged, resulting in predominantly reduced Q_A and increased photoinhibition.

5. Conclusions

Using non-invasive probes of intrinsic pH-indicators as constraints, we were able to estimate the relative lumen pH-responses of the light reactions *in vivo*. Our results are in general agreement with the 'moderate' lumen pH hypothesis [5], in which lumen pH is maintained, under normal conditions, in a range where it can regulate light capture while not damaging the photosynthetic apparatus. The predicted lumen pH (Fig. 9) ranged 7.8 to 5.7 should activate pH dependent antenna down-regulation (q_E), but not damage the photosynthetic machinery, particularly the oxygen evolving complex of photosystem II and plastocyanin, which are pH sensitive [5,8,72,73] below about pH=5.5 (cf. Scheme I in [5]). We suggest that mutations of conditions which prevent this pH regulation will lead to increased photodamage [5]. Substantial and variable contributions of $\Delta\psi$ to *pmf* appear to be needed to sustain sufficient ΔG_{ATP} while maintaining a moderate lumen pH in the range that properly regulates the antenna and electron transfer [4].

The relative responses of q_E and the cyt b_6f complex to lumen pH, governed by their respective pK_a and n_H values, appear to be tuned to minimize buildup of reactive intermediates as electron flow is down-regulated under suboptimal conditions. We propose that the 'lag' in accumulation of Z+A at low ΔpH helps to maximize the efficiency of light capture when photosynthesis is light limited. The sharp increase in Z+A when pH decreases around its apparent pK_a coincides with an increase in q_E, under conditions where light input begins to exceed capacity for LEF or NADPH and ATP consumption. At higher ΔpH, when Z+A accumulation is saturated, the q_E response becomes limited by PsbS protonation. The more gradual PsbS response, due to its lower n_H, allows for fine-tuning of the q_E response over the lower pH range. The onset of q_E appears at a slightly higher lumen pH than down-regulation of the cyt b_6f complex, dissipating excess light energy when the capacity for LEF is slowed.

Finally, we provide reasonable ranges for values of C (the relationship between ECS and $\Delta\psi$), allowing for the first time, quantitative estimates of *pmf* and lumen pH *in vivo*. Our approach is strongly supported by the consistency of responses of Z+A accumulation, PsbS protonation and cyt b_6f turnover as a function of predicted lumen pH, over a wide range of conditions, even with large changes in LEF, proton conductivity at the ATP synthase and partitioning of *pmf* into ΔpH and $\Delta\psi$.

Acknowledgements

The authors would like to thank Drs. Gerald Edwards, Thomas Avenson and John Nishio for stimulating discussions, and Masaaki Komatsu, Fred Henderson, and Willow Foster for

contributions to construction of instrumentation, and Dr. Krishna Niyogi for providing seeds of *Arabidopsis npq2*. The authors would also like to thank the anonymous reviewers for their insightful comments. This work was supported by the U.S. Department of Energy (DE-FG02-04ERl5559).

References

[1] U. Junesch, P. Gräber, The rate of ATP-synthesis as a function of ΔpH and Δψ catalyzed by the active, reduced H^+-ATPase from chloroplasts, FEBS Lett. 294 (1991) 275–278.
[2] P. Müller, X.P. Li, K.K. Niyogi, Non-photochemical quenching. A response to excess light energy, Plant Physiol. 125 (2001) 1558–1566.
[3] D.M. Kramer, T.J. Avenson, G.E. Edwards, Dynamic flexibility in the light reactions of photosynthesis governed by both electron and proton transfer reactions, Trends Plant Sci. 9 (2004) 349–357.
[4] D.M. Kramer, J.A. Cruz, A. Kanazawa, Balancing the central roles of the thylakoid proton gradient, Trends Plant Sci. 8 (2003) 27–32.
[5] D.M. Kramer, C.A. Sacksteder, J.A. Cruz, How acidic is the lumen? Photosynth. Res. 60 (1999) 151–163.
[6] A.B. Hope, P. Valente, D.B. Matthews, Effects of pH on the kinetics of redox reactions in and around the cytochrome *bf* complex in an isolated system, Photosynth. Res. 42 (1994) 111–120.
[7] J.N. Nishio, J. Whitmarsh, Dissipation of the proton electrochemical potential in intact chloroplasts (II. The pH gradient monitored by cytochrome *f* reduction kinetics), Plant Physiol. 101 (1993) 89–96.
[8] A. Krieger, E. Weis, The role of calcium in the pH-dependent control of photosystem-II, Photosynth. Res. 37 (1993) 117–130.
[9] J.A. Cruz, C.A. Sacksteder, A. Kanazawa, D.M. Kramer, Contribution of electric field (Δψ) to steady-state transthylakoid proton motive force (*pmf*) *in vitro* and *in vivo*. control of pmf parsing into Δψ and ΔpH by ionic strength, Biochemistry 40 (2001) 1226–1237.
[10] T.J. Avenson, J.A. Cruz, D.M. Kramer, Modulation of energy-dependent quenching of excitons in antennae of higher plants, Proc. Natl. Acad. Sci. U. S. A. 101 (2004) 5530–5535.
[11] K.K. Niyogi, A.R. Grossman, O. Björkman, Arabidopsis mutants define a central role for the xanthophyll cycle in the regulation of photosynthetic energy conversion, Plant Cell 10 (1998) 1121–1134.
[12] C.A. Sacksteder, M.E. Jacoby, D.M. Kramer, A portable, non-focusing optics spectrometer (NoFOSpec) for measurements of steady-state absorbance changes in intact plants, Photosynth. Res. 70 (2001) 231–240.
[13] D.M. Kramer, A.R. Crofts, Activation of the chloroplast ATPase measured by the electrochromic change in leaves of intact plants, Biochim. Biophys. Acta 976 (1989) 28–41.
[14] T.J. Avenson, J.A. Cruz, A. Kanazawa, D.M. Kramer, Regulating the proton budget of higher plant photosynthesis, Proc. Natl. Acad. Sci. U. S. A. 102 (2005) 9709–9713.
[15] B. Genty, J.-M. Briantais, N.R. Baker, The relationship between the quantum yield of photosynthetic electron transport and quenching of chlorophyll fluorescence, Biochim. Biophys. Acta 990 (1989) 87–92.
[16] D.M. Kramer, G. Johnson, O. Kiirats, G.E. Edwards, New fluorescence parameters for the determination of Q_A redox state and excitation energy fluxes, Photosynth. Res. 79 (2004) 209–218.
[17] J.P. Krall, G.E. Edwards, Relationship between photosystem-II activity and CO_2 fixation in leaves, Physiol. Plant. 86 (1992) 180–187.
[18] X.P. Li, O. Björkman, C. Shih, A.R. Grossman, M. Rosenquist, S. Jansson, K.K. Niyogi, A pigment-binding protein essential for regulation of photosynthetic light harvesting, Nature 403 (2000) 391–395.
[19] C.A. Sacksteder, D.M. Kramer, Dark interval relaxation kinetics of absorbance changes as a quantitative probe of steady-state electron transfer, Photosynth. Res. 66 (2000) 145–158.
[20] E.E. Pfündel, M. Renganathan, A.M. Gilmore, H.Y. Yamamoto, R.A. Dilley, Intrathylakoid pH in isolated pea chloroplasts as probed by violaxanthin deepoxidation, Plant Physiol. 106 (1994) 1647–1658.
[21] D. Siefermann, H.Y. Yamamoto, Light-induced de-epoxidation of violaxanthin in lettuce chloroplasts. III. Reaction kinetics and effect of light intensity on de-epoxidase activity and substrate availability, Biochim. Biophys. Acta 357 (1974) 144–150.
[22] O. Björkman, B. Demmig-Adams, Regulation of photosynthetic light energy capture, conversion, and dissipation in leaves of higher plants, in: E.D. Schulze, M.M. Caldwell (Eds.), Ecophysiology of Photosynthesis, Springer-Verlag, Berlin, 1994, pp. 17–47.
[23] J.A. Cruz, T.J. Avenson, A. Kanazawa, K. Takizawa, G.E. Edwards, D.M. Kramer, Plasticity in light reactions of photosynthesis for energy production and photoprotection, J. Exp. Bot. 56 (2005) 395–406.
[24] H.T. Witt, Energy conversion in the functional membrane of photosynthesis. Analysis by light pulse and electric pulse methods. The central role of the electric field, Biochim. Biophys. Acta 505 (1979) 355–427.
[25] T.J. Avenson, A. Kanazawa, J.A. Cruz, K. Takizawa, W.E. Ettinger, D.M. Kramer, Integrating the proton circuit into photosynthesis: progress and challenges, Plant Cell Environ. 28 (2005) 97–109.
[26] A. Kanazawa, D.M. Kramer, *In vivo* modulation of nonphotochemical exciton quenching (NPQ) by regulation of the chloroplast ATP synthase, Proc. Natl. Acad. Sci. U. S. A. 99 (2002) 12789–12794.
[27] J. Harbinson, C. Hedley, The kinetics of $P\text{-}700^+$ reduction in leaves: a novel in situ probe of thylakoid functioning, Plant Cell Environ. 12 (1989) 357–369.
[28] P. Horton, A.V. Ruban, D. Rees, A.A. Pascal, G. Noctor, A.J. Young, Control of the light-harvesting function of chloroplast membranes by aggregation of the LHCII chlorophyll–protein complex, FEBS Lett. 292 (1991) 1–4.
[29] X.P. Li, A.M. Gilmore, S. Caffarri, R. Bassi, T. Golan, D. Kramer, K.K. Niyogi, Regulation of photosynthetic light harvesting involves intrathylakoid lumen pH sensing by the PsbS protein, J. Biol. Chem. 279 (2004) 22866–22874.
[30] N. Keren, A. Berg, P.J. van Kan, H. Levanon, I.I. Ohad, Mechanism of photosystem II photoinactivation and D1 protein degradation at low light: the role of back electron flow, Proc. Natl. Acad. Sci. U. S. A. 94 (1997) 1579–1584.
[31] E.E. Pfündel, R.A. Dilley, The pH dependence of violaxanthin deepoxidation in isolated pea chloroplasts, Plant Physiol. 101 (1993) 65–71.
[32] N.E. Holt, G.R. Fleming, K.K. Niyogi, Toward an understanding of the mechanism of nonphotochemical quenching in green plants, Biochemistry 43 (2004) 8281–8289.
[33] D.M. Kramer, A.R. Crofts, Control of photosynthesis and measurement of photosynthetic reactions in intact plants, in: N. Baker (Ed.), Photosynthesis and the Environment. Advances in Photosynthesis, Kluwer Academic Publishers, Dordrecht, The Netherlands, 1996, pp. 25–66.
[34] G. Finazzi, F. Rappaport, *In vivo* characterization of the electrochemical proton gradient generated in darkness in green algae and its kinetic effects on cytochrome $b_6 f$ turnover, Biochemistry 37 (1998) 9999–10005.
[35] P. Joliot, A. Joliot, Characterization of linear and quadratic electrochromic probes in *Chlorella sorokiniana* and *Chlamydomonas reinhardtii*, Biochim. Biophys. Acta 975 (1989) 355–360.
[36] P. Bennoun, The present model for chlororespiration, Photosynth. Res. 73 (2002) 273–277.
[37] C. Giersch, U. Heber, Y. Kobayashi, Y. Inoue, K. Shibata, H.W. Heldt, Energy charge, phosphorylation potential and proton motive force in [spinach] chloroplasts, Biochim. Biophys. Acta 590 (1980) 59–73.
[38] G. Noctor, C.H. Foyer, Homeostasis of adenylate status during photosynthesis in a fluctuating environment, J. Exp. Bot. 51 (2000) 347–356 (Special Issue).
[39] H. Seelert, A. Poetsch, N.A. Dencher, A. Engel, H. Stahlberg, D.J. Müller, Structural biology. Proton-powered turbine of a plant motor, Nature 405 (2000) 418–419.
[40] A.R. Portis Jr., R.E. McCarty, Effects of adenine nucleotides and of photophosphorylation on H+ uptake and the magnitude of the H+ gradient in illuminated chloroplasts, J. Biol. Chem. 249 (1974) 6250–6254.
[41] W. Junge, W. Ausländer, A.J. McGeer, T. Runge, The buffering capacity of the internal phase of thylakoids and the magnitude of the pH changes inside under flashing light, Biochim. Biophys. Acta 546 (1979) 121–141.
[42] L.A. Staehelin, Chloroplast structure and supramolecular organization of photosynthetic membranes, in: L.A. Staehelin, C.J. Arntzen (Eds.),

Photosynthesis III Photosynthetic Membranes and Light Harvesting Systems, Springer-Verlag, Berlin, 1986, pp. 1–84.
[43] B. Hille, Ionic channels of excitable membranes, Sunderland, Massachusetts, 1984.
[44] M. Hauser, H. Eichelmann, V. Oja, U. Heber, A. Laisk, Stimulation by light of rapid pH regulation in the chloroplast stroma *in vivo* as Indicated by CO2 solubilization in leaves, Plant Physiol. 108 (1995) 1059–1066.
[45] K. Werdan, H.W. Heldt, M. Milovancev, The role of pH in the regulation of carbon fixation in the chloroplast stroma. Studies on CO_2 fixation in the light and dark, Biochim. Biophys. Acta 396 (1975) 276–292.
[46] D. Heineke, M. Stitt, H.W. Heldt, Effects of inorganic phosphate on the light dependent thylakoid energization of intact spinach chloroplasts, Plant Physiol. 91 (1989) 221–226.
[47] H.Y. Yamamoto, T.O.M. Nakayama, C.O. Chichester, Studies on the light and dark interconversions of leaf xanthophylls, Arch. Biochem. Biophys. 97 (1962) 168–173.
[48] M. Havaux, K.K. Niyogi, The violaxanthin cycle protects plants from photooxidative damage by more than one mechanism, Proc. Natl. Acad. Sci. U. S. A. 96 (1999) 8762–8767.
[49] B. Demmig-Adams, A.M. Gilmore, W.W. Adams 3rd, Carotenoids 3: in vivo function of carotenoids in higher plants, Faseb J. 10 (1996) 403–412.
[50] H.Y. Yamamoto, Biochemistry of the violaxanthin cycle in higher plants, Pure Appl. Chem. 51 (1979) 639–648.
[51] M.J. Delrieu, Regulation of thermal dissipation of absorbed excitation energy and violaxanthin deepoxidation in the thylakoids of lactuca sativa. Photoprotective mechanism of a population of photosystem II centers, Biochim. Biophys. Acta 1363 (1998) 157–173.
[52] C.E. Bratt, P.-O. Arvidsson, M. Carlsson, H.-E. Akerlund, Regulation of violaxanthin de-epoxidase activity by pH and ascorbate concentration, Photosynth. Res. 45 (1995) 169–175.
[53] A. Gisselsson, A. Szilagyi, H.E. Akerlund, Role of histidines in the binding of violaxanthin de-epoxidase to the thylakoid membrane as studied by site-directed mutagenesis, Physiol. Plant. 122 (2004) 337–343.
[54] A. Emanuelsson, M. Eskling, H.E. Akerlund, Chemical and mutational modification of histidines in violaxanthin de-epoxidase from *Spinacia oleracea*, Physiol. Plant. 119 (2003) 97–104.
[55] K.K. Niyogi, O. Björkman, A.R. Grossman, *Chlamydomonas* xanthophyll cycle mutants identified by video imaging of chlorophyll fluorescence quenching, Plant Cell 9 (1997) 1369–1380.
[56] D. Siefermann, H.Y. Yamamoto, NADPH and oxygen-dependent epoxidation of zeaxanthin in isolated chloroplasts, Biochem. Biophys. Res. Commun. 62 (1975) 456–461.
[57] A.M. Gilmore, N. Mohanty, H.Y. Yamamoto, Epoxidation of zeaxanthin and antheraxanthin reverses non-photochemical quenching of photosystem II chlorophyll a fluorescence in the presence of trans-thylakoid delta pH, FEBS Lett. 350 (1994) 271–274.
[58] K.K. Niyogi, X.P. Li, V. Rosenberg, H.S. Jung, Is PsbS the site of non-photochemical quenching in photosynthesis? J. Exp. Bot. 56 (2005) 375–382.
[59] A.M. Gilmore, V.P. Shinkarev, T.L. Hazlett, G. Govindjee, Quantitative analysis of the effects of intrathylakoid pH and xanthophyll cycle pigments on chlorophyll a fluorescence lifetime distributions and intensity in thylakoids, Biochemistry 37 (1998) 13582–13593.
[60] S. Woitsch, S. Romer, Expression of xanthophyll biosynthetic genes during light-dependent chloroplast differentiation, Plant Physiol. 132 (2003) 1508–1517.
[61] J.B.F. Charron, F. Ouellet, M. Pelletier, J. Danyluk, C. Chauve, F. Sarhan, Identification, expression, and evolutionary analyses of plant lipocalins, Plant Physiol. 139 (2005) 2017–2028.
[62] R.C. Bugos, S.H. Chang, H.Y. Yamamoto, Developmental expression of violaxanthin de-epoxidase in leaves of tobacco growing under high and low light, Plant Physiol. 121 (1999) 207–213.
[63] R.C. Bugos, S.W. Chang, H.Y. Yamamoto, Distribution of violaxanthin de-epoxidase during leaf development in tobacco. Plant Physiol. 114 (1997) 415–415.
[64] R.P. Hangarter, N.E. Good, Energy thresholds for ATP synthesis in chloroplasts, Biochim. Biophys. Acta 681 (1982) 397–404.
[65] B. Genty, J. Harbinson, Regulation of light utilization for photosynthetic electron transport, in: N.R. Baker (Ed.), Photosynthesis and the Environment, Kluwer Academic Publishers, Dordrecht, The Netherlands, 1996, pp. 67–99.
[66] W. Haehnel, Photosynthetic electron transport in higher plants, Annu. Rev. Plant Physiol. 35 (1984) 659–693.
[67] K. Asada, The water–water cycle in chloroplasts: scavenging of active oxygens and dissipation of excess photons, Annu. Rev. Plant Physiol. Plant Mol. Biol. 50 (1999) 601–639.
[68] E.M. Aro, I. Virgin, B. Andersson, Photoinhibition of photosystem II. Inactivation, protein damage and turnover, Biochim. Biophys. Acta 1143 (1993) 113–134.
[69] X.G. Zhu, D.R. Ort, J. Whitmarsh, S.P. Long, The slow reversibility of photosystem II thermal energy dissipation on transfer from high to low light may cause large losses in carbon gain by crop canopies: a theoretical analysis, J. Exp. Bot. 55 (2004) 1167–1175.
[70] X.P. Li, P. Müller-Moulé, A.M. Gilmore, K.K. Niyogi, PsbS-dependent enhancement of feedback de-excitation protects photosystem II from photoinhibition, Proc. Natl. Acad. Sci. U. S. A. 99 (2002) 15222–15227.
[71] Y. Munekage, S. Takeda, T. Endo, P. Jahns, T. Hashimoto, T. Shikanai, Cytochrome b_6f mutation specifically affects thermal dissipation of absorbed light energy in Arabidopsis, Plant J. 28 (2001) 351–359.
[72] J.D. Sinclair-Day, M.J. Sisley, A.G. Sykes, G.C. King, P.E. Wright, Acid dissociation constants for plastocyanin in the Cu^{I} state, J. Chem. Soc., Chem. Commun. (1985) 505–507.
[73] J.M. Guss, P.R. Harrowell, M. Murata, V.A. Norris, H.C. Freeman, Crystal structure analyses of reduced (CuI) poplar plastocyanin at six pH values, J. Mol. Biol. 192 (1986) 361–387.